EGYPTIAN ACADEMIC JOURNAL OF
BIOLOGICAL SCIENCES
ZOOLOGY

B

ISSN
2090-0759

WWW.EAJBS.EG.NET

Vol. 17 No. 1 (2025)

Citation: *Egypt. Acad. J. Biolog. Sci. (B. Zoology) Vol. 17(1) pp:87-105 (2025)*
DOI: 10.21608/EAJBSZ.2025.410505

Egypt. Acad. J. Biolog. Sci., 17(1):87-105(2025)

Egyptian Academic Journal of Biological Sciences
B. Zoology
ISSN: 2090 – 0759
Res. Ethics No.: 03-2024-0009
http://eajbsz.journals.ek b.eg/

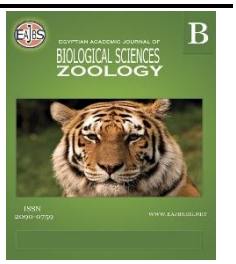

Effect of MYC Knockdown on Autophagy Induction in Breast Cancer Chemo- sensitive and Chemo-resistant Cell Lines

Huda E.E. Yahya[1]; Rokaya H. Shalaby[1]; Shaymaa M.M. Yahya[2]; Nadia N.D. Aniss[1] and Shereen H. B. ElWakeel[1]

[1]Zoology Department, Faculty of women for Arts, Science and Education, Ain Shams University, Asmaa Fahmy Street, Heliopolis, Cairo, Egypt.

[2]Hormones Department, Medical Research and Clinical Studies Institute, and Stem Cell lab, Centre of Excellence for Advanced Sciences, National Research Centre, Dokki, Giza, Egypt.

***E-mail:** hoda.em14@gmail.com ; sherien.elwakeel@women.asu.edu.eg

ARTICLE INFO
Article History
Received:17/12/2024
Accepted:6/2/2025
Available:10/2/2025

Keywords:
Breast cancer, Multidrug resistant, Chemo-resistant, C-MYC, Autophagy.

ABSTRACT

Breast cancer (BC) is the most widespread malignant tumor among women and is the fifth leading cause of cancer mortality. Surgery, radiation, chemotherapy, and immunotherapy are used in combination to treat breast cancer, depending on the stage and type of tumor. Chemo-resistance remains a serious clinical problem in BC management. Currently, the role of autophagy in cancer resistance has become an intense area of investigation. This study aimed to state the impact of c-MYC knockdown on autophagy induction in chemo-sensitive and chemo-resistant breast cancer cells. In order to accomplish the aim of this study, we used two distinct types of breast cancer cell lines. Estrogen sensitive MCF-7 cells, cultured in the presence of tamoxifen (TAM), and a triple-negative MDA-MB 231cell line, cultured in media containing doxorubicin (DOX). Changes in cellular morphology were noticed to have a resistant phenotype at the end of seven passages. Fluorescence microscopy revealed that c-MYC knockdown stimulates autophagy induction in acutely treated MCF-7 cells, elevated in MDR/ MCF-7 cells, and was highest in c-MYC silenced MDR- MCF-7 cells. c-MYC knockdown in MDR-MDA-MB231cells had the strongest emission compared to MDR-negative control (NC) MDA-MB231 cells and acutely treated MDA-MB231cells in both tested groups. qPCR estimated elevation in autophagic-related tested gene in acute tamoxifen-treated c-MYC silenced MCF-7 cells, indicating higher autophagy induction. Repression of c-MYC in TAM resistance MCF-7 cells elevates the expression of all tested autophagy-related genes compared to NC cells. As for MDA-MB231 cells, qPCR estimated increased levels of all tested autophagic-related genes in acute doxorubicin treated cells, conversely, reduction of c-MYC decreased most autophagic related genes expression. Reduction of c-MYC in MDR/ MDA-MB231 cells elevated expression levels of all autophagic tested genes more than MDR/ MDA-MB231(NC) cells. In conclusion, c-MYC knockdown had different autophagic induction effects on breast cancer cells regarding their type in chemo-sensitive cells; it was found to be elevated in MCF-7 cells, while decreased in MDA-MB 231 cells. However, it elevates autophagy in chemo-resistant cells.

INTRODUCTION

Breast cancer (BC) is the most widespread malignant tumor among women, according to the latest global statistics in 2020, BC estimated 2.3 million new cases, representing 11.7% of all cancer cases. It ranks as the fifth leading cause of cancer-related deaths globally, with 685,000 deaths (Sung *et al.,* 2021). BC is a metastatic cancer and consequently can transfer to distant organs such as bone, liver, lung, and brain, which mainly accounts for its incurability (Sun *et al.,* 2017). On the molecular level, breast cancer is a heterogeneous disease, it is classified into three major subtypes based on molecular markers:

estrogen (ER+/-), progesterone (PR+/-) receptors, human epidermal growth factor 2; HER2, (HER2+/-) and triple-negative; lacking by the absence all three molecular markers (Waks and Winer 2019). Two distinct types of breast cancer cell lines were used in this study. The estrogen sensitive MCF-7 cell line, which was cultured in the presence of tamoxifen (TAM), and the triple-negative MDA-231cell line, cultured in media contained doxorubicin (DOX) to obtain acquired drug resistance breast cancer cell lines by long-term treatment of the wild type.MYC, myelocytomatosis, an oncogenic family is deregulated in various tumors; generally linked to poor prognosis of these tumors. MYC amplification is present in 30–50% of high-grade breast cancer and it is often elevated in acquired resistance to anti-cancer therapies. Consequently, MYC amplification can be used as a predictive marker for drug-resistance in breast cancer. As well, targeting MYC effectors could be useful in treating drug resistant, MYC-dependent tumors (Fallah *et al.*, 2017). MYC family members are transcription factors, which are responsible for the regulation of various gene expression. Among them, c-MYC; cellular myelocytomatosis oncogene, is closely related to the progression of tumors. c-MYC gene is located on human chromosome 8, and participates in cell cycle progression, proliferation, apoptosis, and cellular transformation (Gao *et al.*, 2023). Autophagy is a cell protective mechanism that removes damaged proteins and organelles and recycles the degradation products as sources of energy and metabolites in anabolic pathways (Jung, Jeong, and Yu 2020). Autophagy dysfunction is associated with a variety of human pathologies, including lung, liver, and heart disease, neurodegeneration, myopathies, cancer, ageing, and metabolic diseases, such as diabetes (Parzych and Klionsky 2014). However, autophagy is also considered as type II programmed cell death; autophagic cell death (ACD) (Bednarczyk *et al.*, 2018). Yet, the definition and the relationship between autophagy and cell death remain unclear and needs further study to utilize autophagy in the various treatments of human diseases (Jung, Jeong, and Yu 2020).

The steps of macroautophagy are initiation, phagophore elongation, autophagosome maturation, autophagosome fusion with the lysosome, and finally, proteolytic degradation of the contents. Each step is highly conserved; about 30 genes of the autophagy-related genes (ATG) family regulate this process (Bednarczyk *et al.*, 2018). Autophagy can occur in either a selective or non-selective manner. ("bulk") (Hurley and Young 2017). Autophagic selectivity is mediated by autophagy receptors, sequestosome 1 p62/SQSTM1, tethering cargo to the growing phagophore (Mejlvang *et al.*, 2018).

Autophagy initiation involves two protein complexes; the UNC-51-like kinase 1 (ULK1) protein kinase complex and the PI3KC3-C1 lipid kinase complex: class III phosphatidylinositol 3 kinase complex I (Hurley and Young 2017). The ULK1 complex consists of ULK1, ATG13, FIP200, and ATG101.In this complex, the serine/threonine protein kinase; ULK1 is the essential factor in autophagy initiation (Zachari, Longo, and Ganley 2020). ATG13 facilitates the binding of ULK1 to the Phagophore Assembly Site (PAS). Focal adhesion kinase family interacting protein of 200kDa (FIP200); acts as a scaffold that modulates the anchoring of all autophagy-related (ATG) proteins onto the PAS (Angela *et al.*, 2022).

ATG101 is present in the phagophore, responsible for phosphorylating ATG13 and ULK1 (Bednarczyk *et al.*, 2018). Once the ULK complex is formed, it recruits ATG9 vesicles; thought to be the nucleation of autophagosome formation. This complex assembly may also be driven by the soluble autophagy cargo adaptor p62, which forms fluid-like condensates with ubiquitinated proteins and interacts with FIP200 to recruit the ULK complex (Yamamoto, Zhang, and Mizushima 2023). ULK1 complex stimulates phagophore nucleation by activating class III phosphatidylinositol 3 kinase (PI3KC3) complex I (PI3KC3–C1), which includes; class III PI3K, vacuolar protein sorting 34 (VPS34), vacuolar protein sorting 15 (VPS15), p150, Beclin-1 and ATG14. PI3KC3–C1 binds to membranes via ATG14, BECN1 and VPS34, then VPS34 generates PI3P; lipid phosphatidylinositol 3-phosphate (Angela *et al.*, 2022; Yamamoto, Zhang, and Mizushima 2023). PI3P-enriched subdomains of the ER, known as omegasomes. Upon the inception of PI3P, the phagophore begins to elongate into a cup-shaped structure and begins to engulf cellular material (Hurley and Young 2017). The PI3P binds to WIPI proteins (WD Repeat Domain Phosphoinositide-Interacting Protein), which further recruit ATG2, and forms a rod-shaped structure that attaches to the ER membrane and the autophagic membrane. WIPI2 binds to ATG16L1, a component of the ATG12–ATG5–ATG16L1 complex, to promote lipidation of ATG8 proteins (LC3 and

GABARAP family proteins, which are collectively called ATG8)**.** Then ATG8 recruits ATG2; it has an LC3-interacting region (LIR)**.** ATG2 transfers lipids to the outer leaflet of the autophagic membrane, and ATG9 scrambles and translocates phospholipids between the outer and inner leaflets (Yamamoto, Zhang, and Mizushima 2023)**.**

It is also known that, the binding of PI3P to WIPI promotes the separation of the isolation membrane from the ER membrane**.** To continue elongation of the isolation membrane, the PI3KC3 complex binds to the ATG5-ATG12 complex and the ATG8/LC3 (microtubule-associated protein light chain 3), system via WIPI promoting ATG5-ATG12 complex and ATG8/LC3 system ubiquitination until the isolation membrane closes, forming an autophagosome (S. Liu 2023)**.**

Many reports demonstrate that autophagy plays a fundamental part in breast cancer initiation, progression and therapy (Angela *et al.*, 2022)**.**

The present study aims to examine c-MYC knockdown effect on ER+ cell line, MCF-7 as well as TNBC cell line, MDA-MB231**.** We also studied the influence of c-MYC silencing on autophagy in MCF-7 as well as MDA-MB231 cell lines. Quantitative analysis of autophagic genes expression: p62, ATG5, ULK1 and BECLIN1 were done. Additionally, detection of the autophagic vacuoles were studied by fluorescence microscopy. Cells were followed up through experimental time by conventional microscope.

MATERIALS AND METHODS

Cell Culture:

Human breast cancer cell lines, MCF-7 (ATCC: HTB-22), and MDA-MB-231 (ATCC:HT-B26), including the human triple-negative cell line, were sourced from the American Type Culture Collection and commercially obtained from The Holding Company for Biological Products and Vaccines "VACSERA" Egypt. MCF-7 and MDA-MB231 cells were maintained in Dulbecco's modified Eagle's Medium (DMEM) (Biowest, Germany), supplemented by 10 % fetal bovine serum (FBS), 4mM L-glutamine, 100 U/ml penicillin, and 100µg/ml streptomycin sulfate at 37 °C in 5% CO2. When cells were approximately 80% confluent (about 48h), cells were sub-cultured to maintain it in the exponential growth phase.
For the acute experiment, the MCF-7 cells were seeded in a 25T flask in complete growth media containing 1µM of TAM. MDA-MB231 cells were treated with (0.5µM) DOX, for 24h**.** Then cells were treated with a transfection complex with negative control siRNA for NC cells, and silenced c-MYC cells were transfected with 5nM sic-MYC**.** After 24h change transfection media and cells were harvested for different experiments**.**

Multi-Drug Resistance (MDR); Phenotype:

Obtained by maintained cells with non-toxic dose of chemotherapy**.** MCF-7 cells were treated with 1µM TAM, while MDA-MB231 cells were treated with 0.19µM DOX. The cells kept in proper condition; incubated at 37ºC, and 5% CO_2. Then cells were sub-cultured when confluence was about 80%, for several passages to gain acquired drug resistance.

siRNA Design and Sequence:

The small interfering RNA (siRNA) sequence targeting c-MYC (GenBank accession no. NM_002467) was purchased from Qiagen (USA) and corresponds to coding regions of these genes. siRNA was supplied in lyophilized form, and upon delivery, the siRNA (1nmol) was reconstituted with RNase-free water provided by the manufacturer to obtain a stock solution of 20µM.

Cell Transfection with siRNA:

Before transfection, 5×10^5 cells were seeded per well of 6-well plates in DMEM culture medium containing 10 % FBS serum, 10 % L-glutamine, and antibiotics. On day 2, cells were transfected with 5nM sic-MYC in serum-free media using 4µl of the HiPerFect Transfection Reagent (Qiagen, USA). miScript Inhibitor Negative Control, which has no homology to any known mammalian gene, was used as a negative control (NC). On day 3, the media was replaced with fresh, complete media, and the cells were incubated at the proper conditions for another 48 h. On day 5, the cells in the first 6-well plate were harvested using QIAzol reagent and subjected to quantitative real-time PCR (qPCR) analysis for estimating c-MYC gene expression levels. At the end of the experimental period, the other plates were used for further gene expression analysis and microscopic examination.

Morphological Studies:

Conventional microscope is useful for observing living cells at the bottom of a large container under more natural conditions than on a glass slide; hence, they are important in biology and medical research**.** Culturing MCF-7 and MDA-MB231 cells in a culture flask (for acute and MDR experiments), or in a culture plate for experimental use were examine every 24h using a Zeiss, Jana, Germany microscope.

Fluorescence Microscope:

For detecting the autophagic vacuoles (acidic compartment), the lysosomotropic agent acridine orange (AO), a weak base that moves freely across biological membranes when uncharged, was used. Its protonated form accumulates in acidic compartments, where it forms aggregates that fluoresce bright red**.** 1µg AO to 1 ml absolute ethanol and mix well**.** It is stable for 2 weeks at room temperature**.** 25µl of cell suspension was transferred to glass slides, add 1µl AO, and then immediately cells were examined under a fluorescence microscope**.** Cells were investigated using a fluorescence microscope (ZEISS Axiostar Plus microscope; ZEISS, Germany) in the National Research Center, NRC. Excitation wavelength: 502nm; and emission wavelength: 526 nm**.**

Gene Expression Analysis using Quantitative real-time polymerase chain reaction (qPCR):

Total RNA was isolated from MCF-7 or MDA-MB-231 cells using an RNA extraction kit (Thermo Scientific, Fermentas, #K0731) according to the manufacturer's instructions**.** RNA extraction kit containing; Lysis buffer (137 mM NaCl, 2.7 mM KCl, 10 mM Na2HPO4, 2 mM KH2PO4, pH 7.4)**.** Proteinase K solution (to a final concentration of 20 ug/ml), wash buffers I and II, and water, nuclease-free**.**

cDNA synthesis was accomplished using Reverse transcription kits (Thermo Scientific, Fermentas, #EP0451) according to the manufacturer's instructions**.**

qPCR with SYBR Green was used to measure the expression of mRNAs of targeted autophagic related genes in MCF-7, and MDA-MB231 cells**.** The isolated cDNA was amplified using 2X Maxima SYBR Green/ROX qPCR Master Mix following the manufacturer protocol **(**Thermo Scientific, USA, # K0221**)** and gene-specific primers. The primers and primer sequence used in the amplification are listed in Table 1.

Table 1. Primer sequences used for the real-time polymerase chain reaction.

Target gene	Forward sequence	Reverse sequence
P62	5′-GCCAGAGGAACAGATGGAGT-3′	5′-TCCGATTCTG GCATCTGTAG-3′
ATG5	5′-AGCAACTCTGGATGGGATTG-3′	5′-CACTGCAGAGGTGTTTCCAA-3′
ULK1	5′ GGCAAGTTCGAGTTCTCCCG-3′	5′-CGACCTCCAAATCGTGCTTCT-3′
BECN1	5′-GGCTGAGAGACTGGATCAGG-3′	5′-CTGCGTCTGGGCATAACG-3′
c-MYC	5′-GCTGCTTAGACGCTGGATTT-3′	5′-CACCGAGTCGTAGTCGAGGT-3′
GAPDH	5′-GGTGAAGGTCGGAGTCAACG-3′	5′ TGAAGGGGTCATTGATGGCAAC 3′

(P62): SQSTM1 gene, (ATG5): Autophagy Related 5 gene, (ULK1): Unc-51-like autophagy-activating kinases 1, (BECN1): gene encode Beclin-1 protein, (c-MYC) cellular myelocytomatosis oncogene encode MYC proto-oncogene, and (GAPDH): glyceraldehyde-3-phosphate dehydrogenase.

Relative Expression:

The polymerase chain reaction mixture was carried out in a 25 µl, which contains the following: 3µl of cDNA template (10-20 ng/ µl), 12.5 µl of 2X Maxima SYBR Green/ROX qQRT-PCR Master Mix, 1 µl primer forward (10 µM), 1 µl primer reverse (0.1-0.5 µM), 7.5 µl water, nuclease-free**.** The final reaction mixture was placed in a StepOnePlus real-time thermal cycler (Applied Biosystems, Life Technology, USA). Thermal profiles consisted of an initial denaturation at 95˚C for 10 min, followed by 40 cycles of denaturation at 95˚C for15 sec, annealing at 60˚C/ 30 sec, and extension at 72˚C for 30 sec**.** At the end of the last cycle, the temperature was increased from 60 to 95 °C to produce a melt curve. The housekeeping gene (GAPDH) is represented as normalized gene that is used to calculate the relative gene expression or fold change in the target gene**.** Therefore, the quantities critical threshold (Ct) of the target gene were normalized with quantities (Ct) of the housekeeping gene by using the $2^{-\Delta\Delta Ct}$ method (Livak and Schmittgen 2001)**.**

Statistical Analysis:

The statistical analysis was performed using a t-test in acute treated cells; to compare the two tested groups in each cell line (NC vs., sic-MYC), and one-way ANOVA for MDR groups. We used GraphPad Prism 10.4.0 (621) software, where probability value (p) is considered significant when; $p < 0.05$*, $p < 0.01$** and $p < 0.001$***.

RESULTS

Morphological Results:

We regularly observed phenotypic changes in MCF-7 and MDA-MB-231 cells during the development of drug resistance using a conventional microscope (Figs. 1& 2). The images show changes in cell morphology related to cell state. Untreated MCF-7 and MDA-MB-231 cells (Figs. 1a and 2a, respectively) exhibited the typical elongated epithelial cell shape. Following drug treatment, TAM-treated MCF-7 cells (Fig. 1b) and DOX-treated MDA-MB-231 cells (Fig. 2b) appeared weakened and lost cell-to-cell contact. By the end of the experimental period, a multidrug-resistant profile was evident in both MCF-7 and MDA-MB-231 cells (Figs. 1c and 2c, respectively), as the cells became rounder and exhibited increased proliferation.

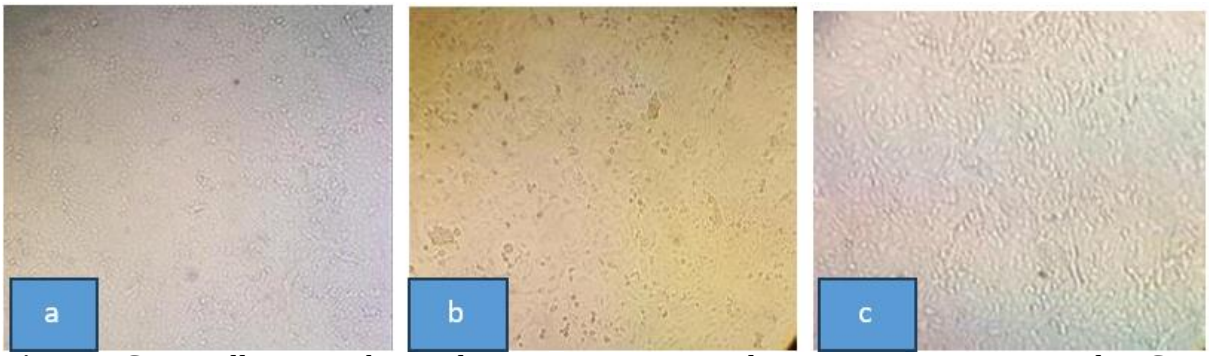

Fig.1: MCF-7 cells were observed using a conventional microscope. a: Untreated MCF-7 cells. Cells show cell-cell contact, with epithelial phenotype, b: Tamoxifen treated MCF7 after the second passage, the cells look tired, and slightly lose cell-cell attachment; due to TAM, treatment**.** c: eighth passage of tamoxifen treated MCF7 cells, the cells look good, more round in shape, signs of transient drug- resistance phenotype**.**

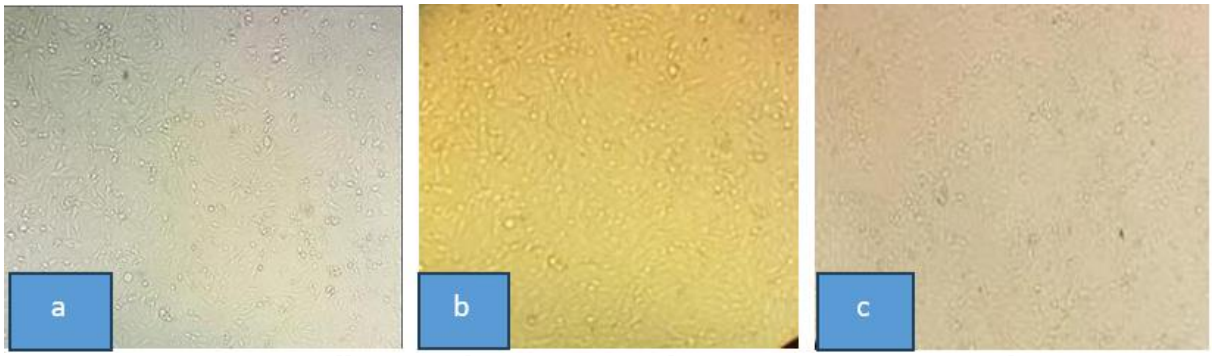

Fig.2: MDA-MB 231 cells' spots by conventional microscope. a: untreated MDA-MB231 cells showing normal elongated shape and cell-cell contact. b: shows the second passage of MDA-MB 231 cells treated and maintained in media containing DOX. Cells look good and well proliferated. c: seventh passage of DOX-treated MDA-MB 231 cells, showing about 80% confluence. Cells look good, well proliferating, and become rounder, referring to drug resistance phenotype cell transformation.

Fluorescence Microscopy Results:

We examined autophagy induction by detecting the presence of autophagic vacuoles using fluorescence microscopy. Acute TAM-treated MCF-7 cells (Fig. 3a) exhibited a slight greenish-yellow emission. However, when c-MYC was silenced in acute TAM-treated MCF-

7 cells (Fig. 3b), the greenish-yellow emission increased, indicating enhanced autophagy induction. In TAM-resistant MCF-7 cells (Fig. 4a), the fluorescent emission shifted to yellow, suggesting an increase in the formation of autophagic vacuoles, particularly in c-MYC-silenced cells (Fig. 4b). Acute DOX-treated MDA-MB-231 cells (Fig. 5a) displayed yellow emission, which was stronger in c-MYC-silenced cells (Fig. 5b). Fluorescence microscopy results revealed that the formation of AVOs (acidic vesicular organelles) increased in DOX-resistant MDA-MB-231 cells (Fig. 6a); however, the yellow emission was more intense in c-MYC-silenced cells, indicating a higher level of AVO formation (Fig. 6b).

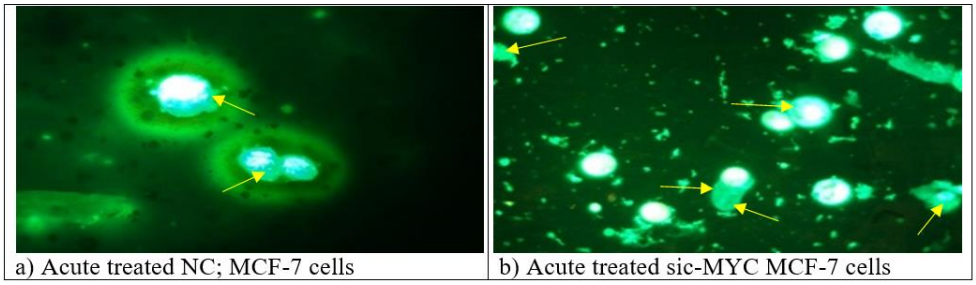

a) Acute treated NC; MCF-7 cells | b) Acute treated sic-MYC MCF-7 cells

Fig.3: Fluorescence microscope image of MCF-7 after stained with AO; (a) AO staining of acute tamoxifen-treated NC; MCF-7 and (b) acute tamoxifen-treated MCF-7 silenced c-MYC gene. Spots show greenish-yellow emission (arrows) in both cell stats; however, the light emission is more in MCF-7 cells silenced c-MYC gene, indicating higher acidic vesicular organelles (AVOs) induction and suggests that these cells were undergoing autophagy.

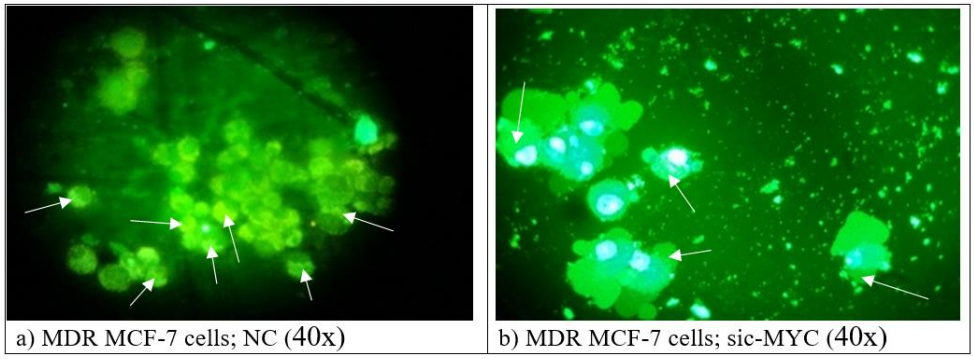

a) MDR MCF-7 cells; NC (40x) | b) MDR MCF-7 cells; sic-MYC (40x)

Fig. 4: Florescence microscopy spots of MDR MCF-7 cells staining with Acridine orange (AO);(a) tamoxifen-resistance MCF-7 cells (NC) and (b) tamoxifen-resistance MCF-7 cells sic-MYC, both types of cells showed numerous greenish-yellow cells, get higher in sic-MYC, signifying the presence of autophagic vacuoles**.**

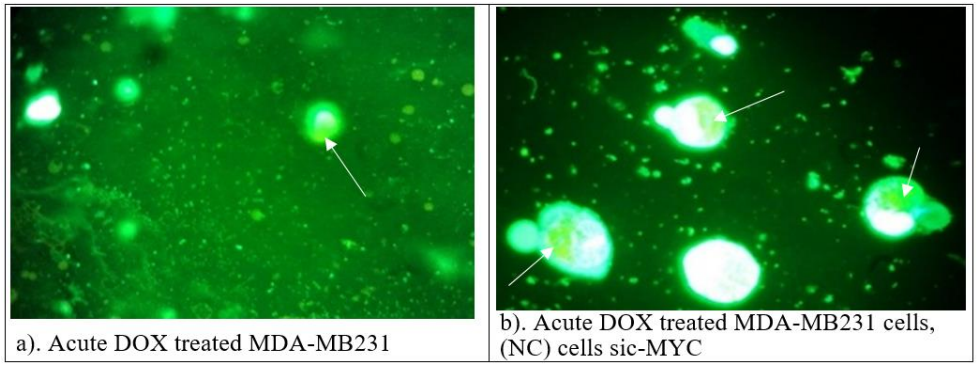

a). Acute DOX treated MDA-MB231 | b). Acute DOX treated MDA-MB231 cells, (NC) cells sic-MYC

Fig. 5: Acutely treated doxorubicin MDA-MB231 cells staining with acridine orange (AO). Figure (a) c-MYC wild-type MDA-MB231 acutely treated doxorubicin (negative control); the white arrow point to yellow emission refers to the presence of some AVOs. Figure (b). c-MYC silenced MDA-MB231; white arrows show red light emission indicting AVOs formation that refers to autophagic induction**.**

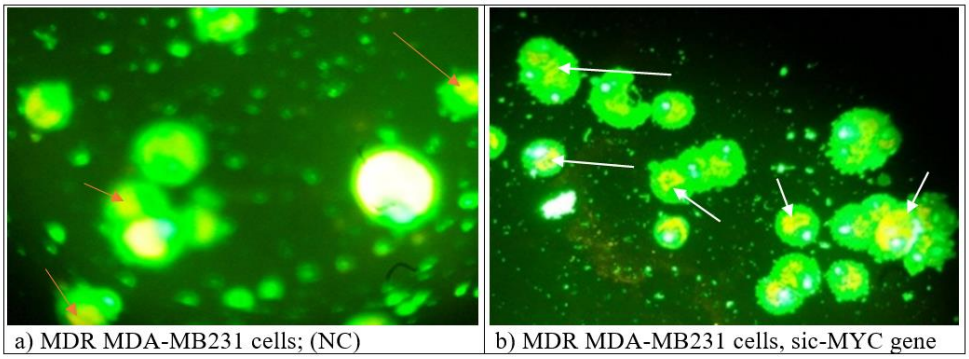

Fig. 6: MDR MDA-MB231 cells staining with acridine orange (AO). (a) MDR MDA-MB231 (NC) cells; orange arrows, show red emission indicating autophagic vacuoles formation. (b): MDR MDA-MB231 sic-MYC cells; white arrows, show strong red emission indicating higher AVOs formation.

qPCR Results:

Tamoxifen acutely treated MCF-7 cells; negative control (NC) *vs.* silenced c-MYC (sic-MYC):

Quantitative real-time PCR was performed to detect changes in the expression of autophagic genes in response to c-MYC silencing in both acute and drug-resistant cells. Figure 7, illustrates the expression levels of different genes (Fig. 7a, b, c, and d) for P62, ATG5, ULK1, and Beclin-1, respectively, in acute TAM-treated MCF-7 cells (NC) compared to acute TAM-treated MCF-7-si-c-MYC cells. The results show varying expression levels of these genes between the two groups, with generally elevated levels in the c-MYC-silenced group. Figure 7f, demonstrates the expression level of the c-MYC gene in NC versus TAM-treated MCF-7-si-c-MYC cells. In TAM-resistant MCF-7 cells (Fig. 8a, b, c, d, and e), the elevation in the expression levels of autophagic genes (P62, ATG5, ULK1, and Beclin-1) was more pronounced in TAM-resistant MCF-7-c-MYC-silenced cells compared to the NC group. Figure 8e, shows the c-MYC expression level in all groups except for the sic-MYC group.

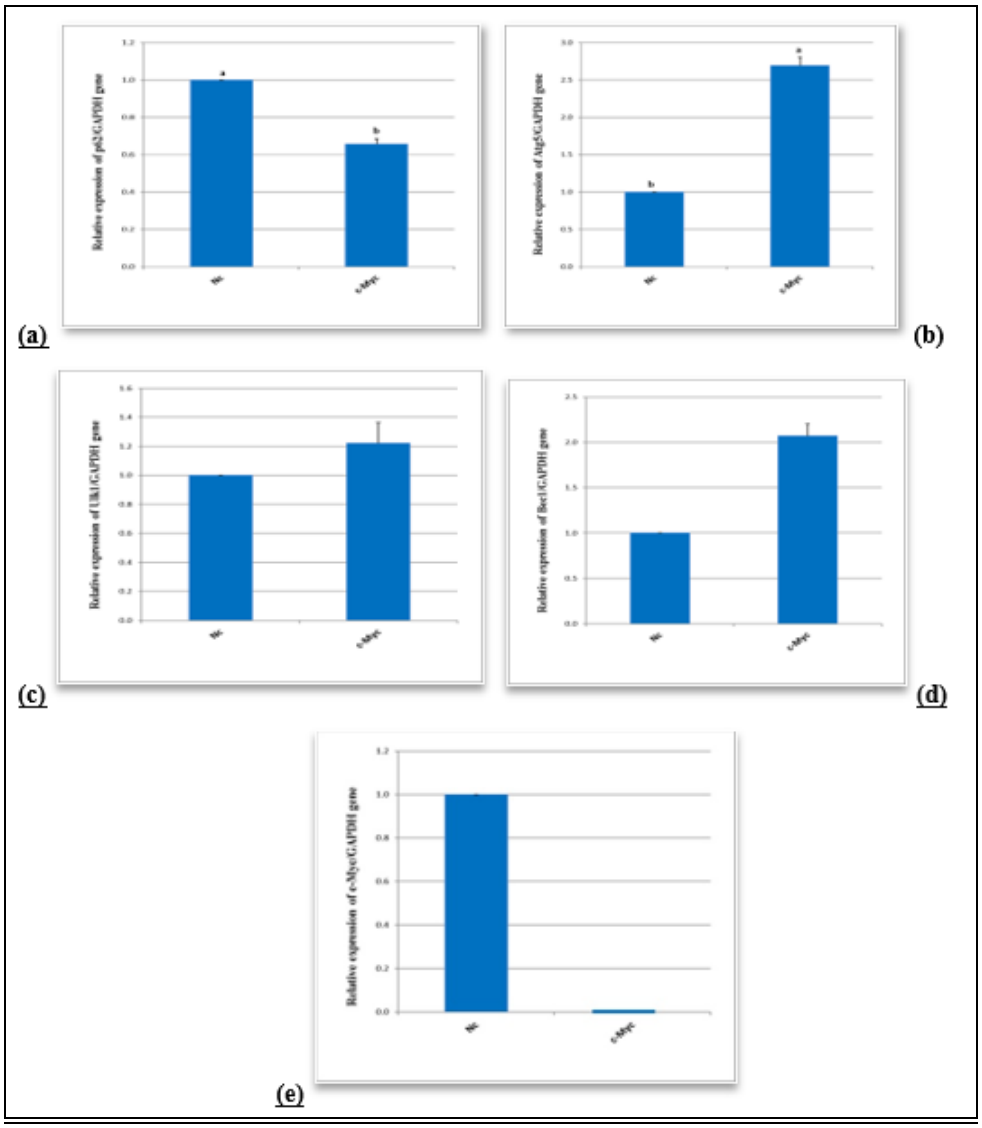

Fig. :7 Graph represents gene expressions by qPCR analysis of acute TAM treated MCF7 NC. vs. sic-MYC cells.Means within columns carrying different superscript letters are significantly different. (a)**:** This graph shows higher p62 expression in acutely treated MCF-7 (NC) cells**.** P=0.0021 (P≤ 0.05)**.** (b)**:** shows differences in the expression levels of the ATG5 gene between acute TAM treated MCF7 (NC) *vs.* sic-MYC cells**;** this difference was significantly different**;** (P≤ 0.05)**,** as P=0.0017**.** (c)**:** shows differences in ULK1 levels, and it is higher in acute treated MCF7 cells with sic-MYC gene (P= 0.0129)**.** (d)**:** The graph shows difference in the expression level of the Beclin-1 gene between NC. *vs.* sic-MYC acute TAM treated MCF-7 cells P= 0.0039**.** (e)**:** The graph shows differences in the expression between; NC. *vs.* sic-MYC, of acute TAM treated MCF-7 cells**;** as fold change in the NC group (1.0) and the fold change in the sic-MYC group (0.0), show difference in gene expressions between the two tested groups**.**

MDR-MCF7 Cells:

In TAM-resistant MCF-7 cells (Fig. 8a, b, c, and d), for P62, ATG5, ULK1, and Beclin-1, respectively, we detected elevated expression levels of autophagic genes, predominantly in TAM-resistant MCF-7-c-MYC-silenced cells compared to the NC group. Figure 8e shows the c-MYC expression level in all groups except for the sic-MYC group.

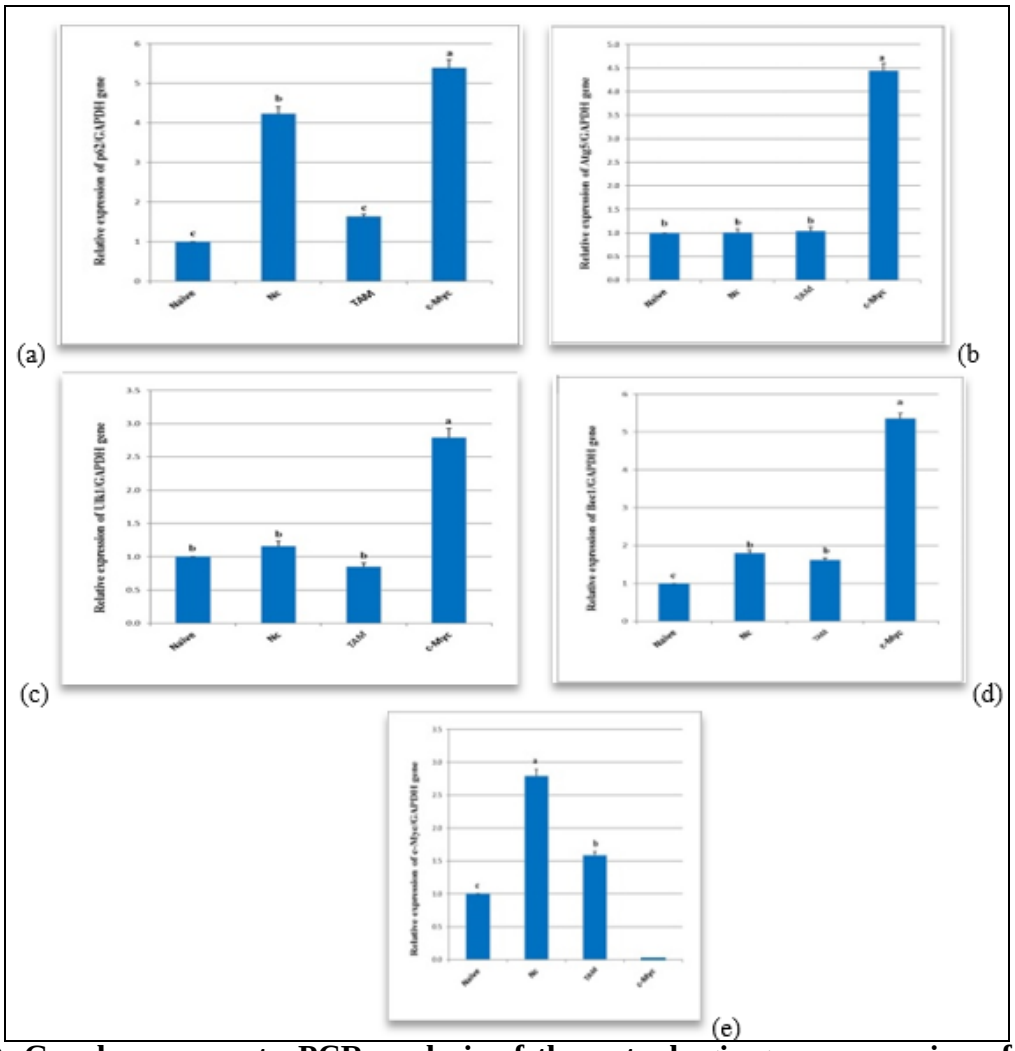

Fig. (8). Graphs represent qPCR analysis of the autophagic gene expression of MDR-MCF7; NC. vs. sic-MYC, cells. Means within columns carrying different superscript letters are significantly different; there is a significant difference between group take (a) and group named (b) as well as between (a, b) and (c) referred group**.** (a): Diagram shows difference in the expression levels of the ATG5 gene between acute TAM-treated MCF7 (NC) vs. sic-MYC cells**;** this difference was significant (P≤ 0.05)**,** as (P = 0.0001)**.** (b)**:** The figure clearly shows an obvious elevation in ATG5 expression in sic-MYC drug-resistant MCF7 cells. P= 0.0001, which is considered significantly different**.** (C)**:** Graph shows obvious difference in ULK1 expression levels among different groups; however, it is higher in c-MYC repressed drug-resistant MCF7 cells**.** qPCR results show a P Value P=0.0001, which is considered significantly different**.** (d): The diagram shows differences in expression levels of the BECLINE gene in different tested groups; however, BECLIN expression is higher in sic-MYC drug-resistant MCF7 cells (P value =0.0001), which is considered significantly different (P≤ 0.05)**.** (e)**:** Means within columns carrying different superscript letters are significantly different (P≤ 0.05). The graph shows c-MYC significant increase in c-MYC expression in TAX-treated cells; took letter (b) than naïve parental cells; get (c) letter**.** Moreover, (NC) MDR-MCF7 cells have significantly the highest c-MYC expression; referred to as (a)**.**

MDA-MB 231 Cells:

Doxorubicin Acute Treated (NC) *vs.* (sic-MYC) MDA-MB231 Cells:

To identify the effect of c-MYC silencing on acute DOX-treated MDA-MB-231 cells, Figures 9a, c, and d, show decreased gene expression levels of P62, ULK1, and Beclin-1, respectively, in the c-MYC-silenced group, except for ATG5 (Fig. 9b), which exhibited nearly the same expression level in both tested groups. Figure 9e demonstrates the reduction in c-MYC gene expression in the sic-MYC group compared to the NC group.

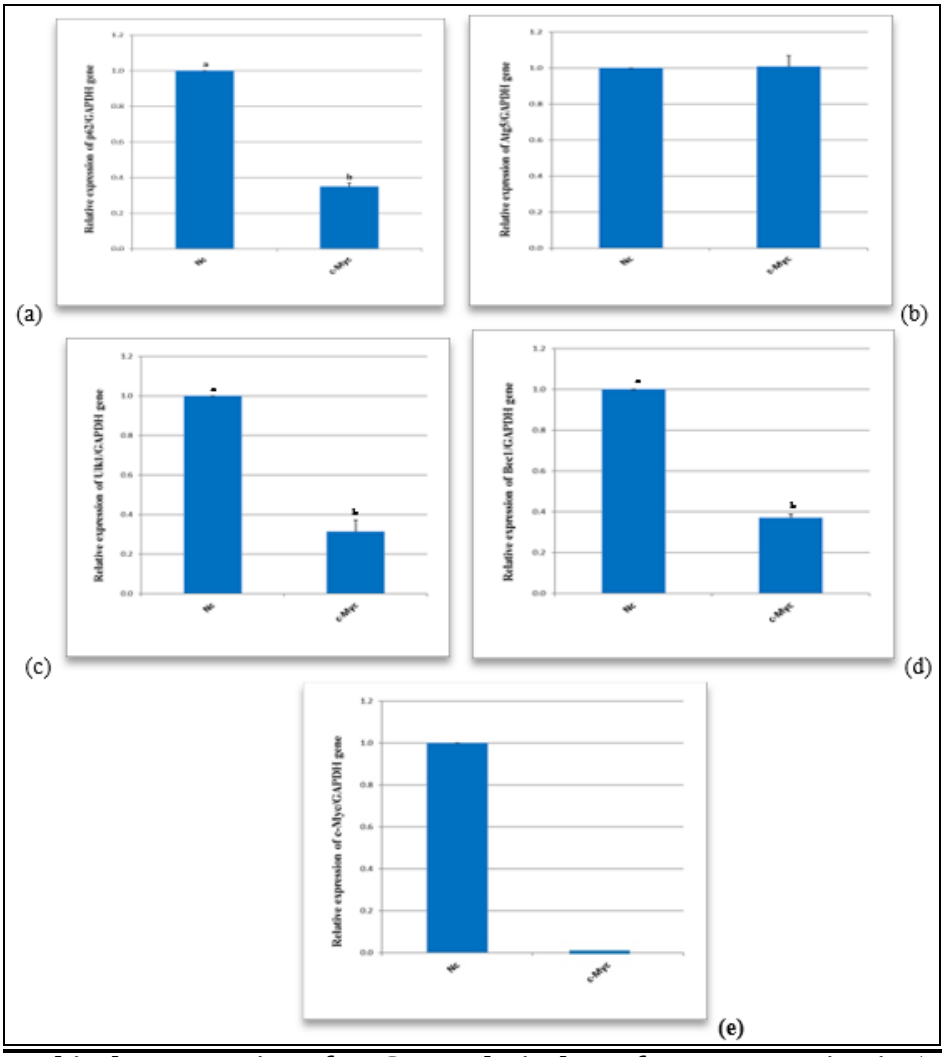

Fig. (9). Graphical presentation of qPCR analysis data of gene expression in (NC) *vs.* sic-MYC of acute DOX treated MDA-MB 231.

Means within columns carrying different superscript letters are significantly different (P≤ 0.05)**.** (a): The graph shows significant differences (P= 0.0032) in P62 gene expression between (NC) and sic-MYC of acute DOX treated MDA-MB 231**.** (b): Graph shows almost equal expression levels of the ATG5 gene in acute DOX-treated cells in both (NC) and sic-MYC in MDA-MB231 cells**,** P Value is considered non-significant, which means there is no statistical difference between the expression levels of the ATG5 gene in both tested groups**.** (c): qPCR results of the ULK1 gene in acute DOX-treated MDA-MB231 cells show difference in the expression level between (NC) and sic-MYC acute DOX-treated MDA-MB231 cells; as NC cells have higher ULK1 gene expression**.** Data was estimated by a two-tailed unpaired t-test; showing P value (P= 0.0355), which is considered significant, between the two tested groups**;** (NC) and sic-MYC of acute DOX-treated MDA-MB231 cells**.** (d)**:** Representing difference in the expression level of the BECLIN1 gene and it is higher in the case of NC acute DOX-treated MDA-MB231 cells**.** Calculation of P value by two-tailed unpaired t-test shows P value = 0.0029, which is considered significant, between (NC) and repressed c-MYC gene of acute DOX-treated MDA-MB231 cells**.** (e)**:** In acute DOX-treated MDA-MB 231 cells, the level of c-MYC gene expression was decreased in sic-MYC cells**.** In contrast, there was a difference in the c-MYC gene expression level between the sic-MYC and NC groups, but this difference was not statistically significant (Fig 9 e).

qPCR Results of MDR/ MDA-MB231 (NC) *vs.* sic-MYC **Cells:**

The differences in the expression levels of the autophagy-related genes P62, ATG5, ULK1, and Beclin-1 were detected in Figures 10a, b, c, and d, respectively, showing

increased expression levels of all tested genes. Figure 10e shows c-MYC expression levels in different groups and demonstrates reduced c-MYC expression in the sic-MYC group, indicating enhanced autophagy induction.

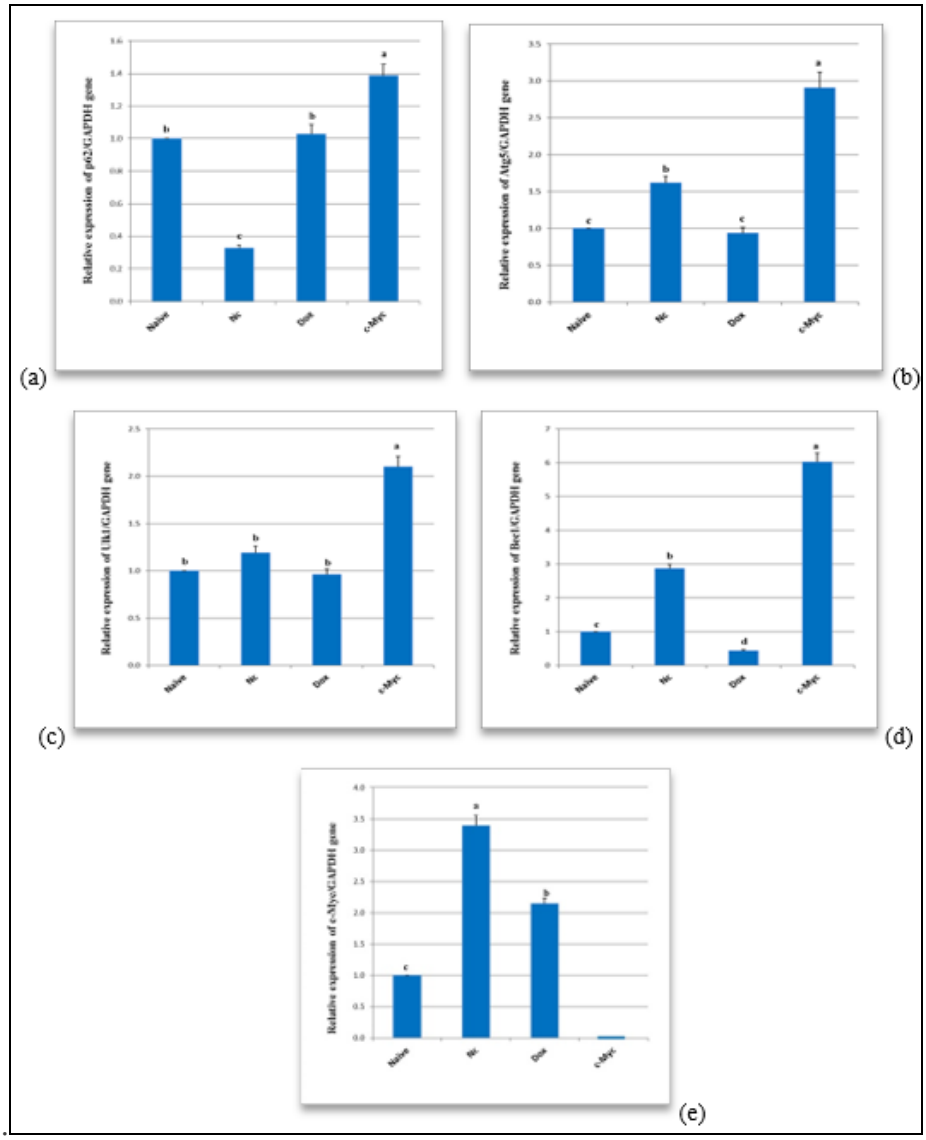

Fig. (10). qPCR graphical presentation of the autophagic gene expression of MDR/ MDA-MB231 (NC) *vs*. silenced c-MYC **cells.**

Means within columns carrying different superscript letters are significantly different (P≤ 0.05). A one-way ANOVA statistical analysis was used to determine the significance between negative control (NC) and sic-MYC samples. **(a):** The P62 gene shows different expression levels in tested groups it was lower in the NC group; letters shown in the graph indicates significant expression differences between, the sic-MYC group, the naïve and DOX naive treated cells and NC group (P = 0.0001)**. (b):** ATG5 gene expression was increased in the NC group, however, it was significantly increased in sic-MYC group**.** P = 0.0001 show there is statistical significance between NC and sic-MYC groups**. (c):** This chart shows ULK1 gene expression in DOX-resistant MDA-MB231; NC. *vs.* sic-MYC cells**.** The graph representing elevation in the expression level of the ULK1 in c-MYC repression cells shows a P value of 0.0001, which is considered significantly different**. (d):** The chart shows an elevation in the BECLIN gene in c-MYC silenced cells than in other tested groups**.** A one-way ANOVA statistical analysis of these data shows P value (0.0001) of the BECLIN1 gene in DOX-resistant MDA-MB231; NC. vs. sic-MYC, cells, which is supposed to have a significant difference**. (e):** The diagram shows significant (0.0001) elevation of c-MYC expression in the NC group compared with the other groups**.**

DISCUSSION

In order to propagate MDR we used the acquired mechanism, through cell line exposure to chronic chemotherapy. Inverted microscopy was used to check and follow up morphological changes in experimental cells. Untreated cells had a good proliferation state during the experiment time. On the other hand, treated cells had different fluctuation responses. Untreated MCF-7 cells exhibited an epithelial phenotype; cells were grown as monolayers with strong cell-cell adhesions, round or elongated in shape. This was in consistency with other 2D and 3D studies of MCF7 morphology (Cavo *et al.*, 2016; H. Wang *et al.*, 2017). In parallel, continued expression of MCF7 cells to TAM was performed to confer acquired TAX resistance. Subsequent passages of cells with lose cell-to-cell contacts begin a remodeling of the cytoskeleton and take an elongate shape, indicating a TAX-resistance phenotype. This was consistent with Qi Wang and his co-worker through dose-and time-dependent analyses (Q. Wang, Gun, and Hong 2019). Untreated MDA-MB-231 cells, along with chronic DOX-treated MDA-MB231, had good performance and well proliferated. However, chronic DOX-treated MDA-MB231 cells went through variable behavior of weakness after the fourth passage, recovered, then went back to proliferate again. They both exhibited two morphologically distributed phenotypes: first, polygonal, flattened cells comparable to an epithelial phenotype (Debnath, Gammoh, and Ryan 2023) and second, mesenchymal spindle elongated shaped cells, representing the expression of EMT (S. Liu 2023)**.** Elongated spindle-shaped cells were more obvious in DOX-treated cells and increased with each passage during experimental time. These findings were supported by scanning electron microscopy micrographs of MDA-MB-231 cells, in a study that assumed increasing of "funnel" elongated shape invasion cells in acquired drug resistance cells than wild parental type(Franchi *et al.*, 2020)**.** Spots of the inverted microscope also showed that the sensitive MDA-MB-231 cells have a larger morphology than the drug-resistant MDA-MB-231 cells**.** This is consistent with Yiting Chen and coworkers, observations (Y. Chen *et al.*, 2022)**.**

Autophagic vacuoles formation upon treatment with TAM or TAM conjugated with c-MYC knockdown was evaluated by cellular staining with Acridine Orange (AO)**.** AO itself is a cell-permeable green fluorophore that can be protonated and trapped in acidic vesicular organelles (AVOs), such as autolysosomes. Additionally, it was assumed that AO staining is a quick, accessible and reliable method to assess the volume of AVOs, which increases upon autophagy induction. It was also found that AO metachromatic shift to red fluorescence is concentration-dependent (Thomé *et al.*, 2016)**.** The results of AO show that TAM-treated MCF7 (NC) cells and c-MYC downregulated (sic-MYC) cells underwent autophagy, which indicates that TAM was able to stimulate autophagy, however, c-MYC knockdown increased the ability of TAM to enhance autophagy process**.** These results were supported by Chiara Actis and coworkers who demonstrated that TAX treatment increased autophagic flux, and it started early during TAX treatment and remained elevated during recovery (Actis, Muzio, and Autelli 2021)**.** However, these results are not consistent with the finding that MYC suppression inhibits autophagosome formation and impairs the clearance of autophagy substrates (Toh *et al.*, 2013). As for TAM-resistant MCF7cells the AO staining results show greater autophagic vacuoles induction**.** These results are matched by the fact that autophagy is a key player in drug resistance and that tamoxifen-resistant MCF7 cells show an increased autophagic flux (Actis, Muzio, and Autelli 2021)**.** Increased light emission after c-MYC knockdown indicates a higher level of autophagy induction in tamoxifen-resistant MCF7cells. These results are in agreement with the former study which used human papillomavirus (HPV)-positive head and neck cancer (HNC), HPV-positive HNC. It disclosed that c-MYC knockdown resulted in upregulation of autophagic and lysosomal genes as increasing at the protein level of autophagic markers in different cell lines (Medda *et al.*, 2023)**.**

As for AO staining MDA-MB 231 cells, fluorescence microscopy images confirmed autophagosomes formation in both experimentally treated cells; however, autophagy is obvious and emits a yellow color in c-MYC repressed cells. The expression of autophagy in MDA-MB-231 cells following DOX was evaluated and confirmed to have a cytoprotective role in MDA-MB-231 cells (Loh *et al.*, 2022). DOX is a pleiotropic anticancer, it has the capability of DNA damage, reactive oxygen species (ROS) production, senescence, and the most important to this study its involvement in apoptosis, and autophagy induction (Kciuk *et al.*, 2023). That may explain the fluorescence microscopy data, which point to autophagy

induction in DOX-treated cells.

On the other hand**,** AO staining of DOX acutely treated MDA-MB 231 cells combined with c-MYC inhibition, shows yellow light emission indicating the presence of autophagosome vacuoles. This result is supported by another c-MYC knockdown study showing its effect on autophagy induction elevation(Annunziata *et al.,* 2019)**.** Though it conflicts with the hypothesis that c-MYC inhibition or knockdown inhibits autophagy in MDA-MB 231 cells(Toh *et al.,* 2013) **.** However, that may be due to the effect of DOX in autophagy induction (Kciuk *et al.,* 2023)**.**

Additionally, fluorescence microscopy results show higher autophagic induction in MDR-MDA-MB 231 cells after c-MYC knockdown than any other experimental MDA-MB231 cell type indicating the obvious influence of c-MYC knockdown on DOX-resistant MDA-MB 231 cells. Ida Annunziata, and co-workers had revealed that reduction of MYC levels displaces MYC from E-Box promoter sites of lysosomal and autophagy genes, which grants occupancy of the same sites to MIT/TFE members and results in activation of lysosomal biogenesis and autophagy in Hela cells (Annunziata *et al.,* 2019). Moreover, c-MYC repression is responsible for the autophagic cell death in MYC-expressing diffuse large B-cell lymphoma (DLBCL), through inhibition of c- MYC –mediated aerobic glycolysis and activation of the AMPK/mTOR signaling pathway (Ma *et al.,* 2023)**.**

Attending to figure out the cellular autophagic response to c-MYC silencing, qPCR was used to estimate four major autophagic-related gene levels**.** All tested genes: p62, ATG5, ULK1, BECLIN1, and c-MYC were expressed in all tested cells**.**

qPCR results show that the c-MYC gene expression was higher in drug-treated MCF-7 and MDA-MB231 cells than untreated cells and significantly higher in drug-resistance cells. These results is consistent with another study noticed that the expression level of c-MYC was increased after Eve-Rh2 treatment in lung cancer cell lines NCI-H1975 and HCC827 and in tumor tissues in *in vivo* experiments (Su *et al.,* 2022)**.** The study results are agreed with **Lee *et al.,*** who found 65 higher expression of c- MYC level in TNBCs after chemotherapy compared to untreated cells (Hutchinson *et al.,* 2018)**.** These observations were also supported by another study demonstrated that c- MYC expression in the parental cells was weak then increased significantly in the acquired resistant MCF-7cells (R. Chen *et al.,* 2020)**.** Moreover, Cheng et al. confirmed a higher level of c-MYC gene expression in the tamoxifen-resistant cell line MCF-7/TAM compared to TAM-sensitive MCF-7 cells**.** They supposed that, the role of ERα was replaced by c-MYC as they had function similarities**,** and that down-regulation of the c-MYC protein level re-sensitized the cells to TAM (Cheng *et al.,* 2017)**.**

Concerning autophagy related genes; p62, ATG5, ULK1, and BECLIN1, the qPCR results of acutely treated MCF-7 used in this study revealed an increase in the expression of all tested autophagic related genes in response to c-MYC reduction, except for P62 which was higher in TAM acute treated MCF-7 with wiled c-MYC gene**.** These results are agreed with the finding that, p62 levels are inversely correlated with autophagy activity; the lower the p62 levels, the higher the autophagy flux**.** p62 levels were increased in MCF-7 cells treated with TAM plus Tetrandrine, which potentiates the pro-apoptotic effect of TAM through inhibition of autophagy (Y. Wang *et al.,* 2021)**.**

As for TAM resistance (TAM-R) MCF-7 cells, qPCR data show that MCF7-TamR with negative control cells had higher levels of all tested genes than acutely treated and untreated MCF-7 cells, except for the Atg5 gene, which had almost the same expression level in all the above-mentioned cells**.** This observation is consistent with Chiara Actis and his coworkers, who found that the expression of the Atg5 was unchanged between parental and tamoxifen-resistant MCF-7 cells despite of the increased autophagic flux in tamoxifen-resistant cells (Actis, Muzio, and Autelli 2021)**.** However, this positive expression of ATG5 was associated with TAM-R and poor prognosis of breast cancer, moreover, ATG5 knockdown caused decrease in the proliferation and migration of tamoxifen-resistant breast cancer cells (Zhang *et al.,* 2024)**.**

Current qPCR results also declare that repression of the c-MYC in TAM-R MCF-7 cells, induced in this study, elevates the expression of all tested autophagy related genes: p62, ATG5, ULK1, and BECLIN1**.** These results are in consistent with Junxia Liu and coworkers, who found a higher autophagy induction, and confirmed the involvement of autophagy in the process of developing tamoxifen resistance, they found that the basal level of p62 is higher in TAM-R than it is in MCF-7 (J. Liu, Yue, and Chen 2019)**.** Moreover, the Beclin-1 level was

found to be higher in the TAM-R cell lines compared with the MCF-7 sensitive cell line, suggesting that the degree of autophagy was higher in the TAM-R cells (J. Liu, Yue, and Chen 2019; Y. Wang *et al.,* 2021)**.**

It was revealed that p62 plays a role in regulating, the development and progression of cancer(Lei *et al.,* 2020)**.** As p62 is not only a cargo receptor for autophagy but also a central signalling core, linking several important pro- and anti-inflammatory pathways, p62 activates mTOR, which controls cell proliferation and differentiation; in addition, p62 acts as a positive regulator of the transcription factor NF-κB, which plays a central role in inflammation and cancer development (Hennig *et al.,* 2021)**.**

The results are also in agreement with Annunziata *et al.* (2019) who disclosed that silencing of MYC in HeLa cells led to a statistically significant increase in the expression of several autophagy genes**.** The reduction of c-MYC increased the binding of transcription factor EB (TFEB) to the promoter of different autophagy and lysosomal genes, inducing their activation, particularly in HPV positive head and neck cancer cell lines. In contrast, c-MYC overexpression, competed with these transcription factors resulting in the downregulation of autophagy genes, including p62 and, Beclin-1, thus confirming the c-MYC's role in repressing autophagy.(Medda *et al.,* 2023)**.** Balakumaran et. al. (2009) found that MYC overexpression limits autophagy induction in prostate cancer cell lines; DU145, LNCaP and PC3, through abrogates sensitivity to rapamycin**.**

As for MDA-MB231 cells, qPCR estimated that acute DOX treatment increased levels of all tested autophagic related genes, however, reduction of c-MYC decreased most autophagic related genes expression; P62, ULK1 and BECLIN1 except for ATG5 has the same expression level as in NC cells**.**

These results are consistent with a previous work that used human embryonic kidney (HEK293) cells, which found that MYC knockdown mediated autophagy dysfunction and impaired autophagosome formation (Jahangiri *et al.,* 2021)**.** Along with inhibition of autophagosome formation, MYC depletion impairs the clearance of autophagy substrates**,** via the reduction of c-Jun N-terminal kinase 1 (JNK1)**,** hence decreasing BECLIN1 activity (Toh *et al.,* 2013)**.** Inhibition of autophagy was found to sensitize MDA-MB-231 and MCF-7 to DOX (Aydinlik *et al.,* 2017; Loh *et al.,* 2022) **.** It was found that, DOX localizing Bcl-2 to the nucleus**,** which associated with a pro-apoptotic function (Lovitt, Shelper, and Avery 2018)**.**

Resistant MDA-MB231 cells had a different autophagic responses due to c-MYC knockdown than of acutely treated, silenced c-MYC cells**.** Current qPCR data estimated that the reduction of c-MYC had elevated expression levels of all autophagic tested genes and were much higher than MDR cells with active type c-MYC gene**.** These results are in accordance with the fluorescence microscopy images of this study**.** Our findings are further supported by Medda e*t. al.* (2023) who revealed that the knocking-down of c-MYC upregulates autophagic and lysosomal genes in HPV-positive HNC cells, as well as the increase of autophagic markers at the protein level**.**

Conclusions

The results of this study suggest different effects of c -MYC knockdown on breast cancer cells**.** Estrogen sensitive MCF-7 cell line showed higher expression of autophagic related genes; p62, ATG5, ULK1, and BECLIN1 in response to c-MYC reduction in both Tamoxifen-acute treated and Tamoxifen-resistant MCF-7cells, suggesting a higher degree of autophagy induction**.** While DOX acutely treated triple-negative MDA-MB231cells had decreased most autophagic related genes expression; P62, ULK1, BECLIN1in response to c-MYC reduction**.** On the contrary, DOX-resistant MDA-MB231 cells estimated an increase in the expression levels of all autophagic tested genes in response of c- MYC knockdown, and were much higher than MDR/ MDA-MB231 cells with active type c-MYC gene (NC)**.** From all the above mentioned, we conclude that c- MYC had different responses in breast cancer cells according to the type of breast cancer and cell sensitivity to chemotherapy**.**

Recommendation

Chemotherapy accompanied by c-MYC silencing is a promising strategy; that may be fruitful in re-sensitize chemo-resistance BC**.** More studies on autophagy; as an alternative cell death pathway, in cancer with defective apoptotic cell death program**.**

List of abbreviations

Breast cancer	BC
Estrogen	ER
Progesterone	PR
Human epidermal growth factor 2	HER2
Tamoxifen	TAM
Doxorubicin	DOX
Myelocytomatosis oncogene	MYC
Cellular myelocytomatosis oncogene	c-MYC
Autophagic cell death	ACD
Autophagy-related genes	ATG
SQSTM1	P62
UNC-51-like kinase 1	ULK1
Focal adhesion kinase family interacting protein of 200 kDa	FIP200
Phagophore Assembly Site	PAS
Class III phosphatidylinositol 3 kinase	PI3KC3
Class III phosphatidylinositol 3 kinase complex I	PI3KC3–C1
Vacuolar protein sorting 34	VPS34
Phosphatidylinositol 3-phosphate	PI3P
WD Repeat Domain Phosphoinositide-Interacting Protein	WIPI
Microtubule-associated protein light chain 3	LC3
Biological Products and Vaccines	VACSERA
Dulbecco's modified Eagle's Medium	DMEM
Fetal bovine serum	FBS
Multi-drug resistance	MDR
Negative control	NC
Small interfering RNA	si-RNA
Acridine orange	AO
National research center	NRC
Reverse Transcriptase Polymerase Chain Reaction	RT-qPCR
Quantitative real time Polymerase Chain Reaction	qPCR
Ribonucleic acid	RNA
Complementary Deoxyribonucleic acid	cDNA
Autophagy related gene 5	ATG5
Gene encode Beclin-1 protein	BECN1
Glyceraldehyde-3-phosphate dehydrogenase	GAPDH
Critical threshold	CT
Probability value	p-value
silenced c-MYC	sic-MYC
Acidic Vesicular Organelles	AVOs
Human Papillomavirus	HPV
Head and neck cancer	HNC
Reactive oxygen species	ROS
Microphthalmia-associated transcription factor or melanocyte-inducing transcription factor/ Transcription factor E	MIT/ TFE
Diffuse large B-cell lymphoma	DLBCL
Adenosine monophosphate-activated protein kinase/ mammalian target of rapaMYCin	AMPK/mTOR
Tamoxifen resistance	TAM-R
Human embryonic kidney	HEK293
c-Jun N-terminal kinase 1	JNK1

Declarations:

Ethical Approval: This article does not contain any studies with human participants or animals performed by any of the authors.

Competing interests: The authors declare that there is no conflict of interest.

Author's Contributions: HEEY conducted the experiments, analyzed the results, prepared

the figures, and contributed to the manuscript drafting. RHS, SMMY, NNDA and SHBE had prepared, revised the original manuscript draft and designed the study. All authors reviewed and approved the final manuscript and have provided their consent for publication.

Funding: This work received financial support by STDF, Egypt, innovation grant (grant no. 34789) project to author Shaymaa MM Yahya.

Availability of Data and Materials: The data utilized and analysed during this study are available upon reasonable request from the corresponding author.

Acknowledgments: Not applicable

REFERENCES

Actis, Chiara, Giuliana Muzio, and Riccardo Autelli.,(2021). Autophagy Triggers Tamoxifen Resistance in Human Breast Cancer Cells by Preventing Drug-Induced Lysosomal Damage. *Cancers*, 13(6), pp. 1–23. doi:10.3390/cancers13061252.

Angela, Veronica, Maria Vitto, Silvia Bianchin, Alicia Ann Zolondick, Giulia Pellielo, Alessandro Rimessi, Diego Chianese.,(2022). Molecular Mechanisms of Autophagy in Cancer Development , Progression , and Therapy. *biomedicines* ,(July). doi.org/ 10.3390/biomedicines10071596

Annunziata, Ida, Diantha van de Vlekkert, Elmar Wolf, David Finkelstein, Geoffrey Neale, Eda Machado, Rosario Mosca.,(2019). MYC Competes with MiT/TFE in Regulating Lysosomal Biogenesis and Autophagy through an Epigenetic Rheostat.*Nature Communications*, 10(1).doi:10.1038/s41467-019-11568-0.

Aydinlik, Seyma, Merve Erkisa, Buse Cevatemre, Mehmet Sarimahmut, Egemen Dere, Ferda Ari, and Engin Ulukaya.,(2017). Enhanced Cytotoxic Activity of Doxorubicin through the Inhibition of Autophagy in Triple Negative Breast Cancer Cell Line. *Biochimica et Biophysica Acta - General Subjects*, 1861(2), pp. 49–57. doi:10.1016/j.bbagen.2016.11.013.

Balakumaran, Bala S, Alessandro Porrello, David S Hsu, Wayne Glover, Adam Foye, Janet Y Leung, Beth A Sullivan, et al., (2009). MYC Activity Mitigates Response to RapaMYCin in Prostate Cancer through Eukaryotic Initiation Factor 4E – Binding Protein 1 – Mediated Inhibition of Autophagy. *Molecular Biology, Pathobiology, and Genetics*, (19), pp. 7803–11. doi:10.1158/0008-5472.CAN-09-0910.

Bednarczyk, Martyna, Nikola Zmarzły, Beniamin Grabarek, Urszula Mazurek, and Małgorzata Muc-Wierzgoń., (2018). Genes Involved in the Regulation of Different Types of Autophagy and Their Participation in Cancer Pathogenesis. *Oncotarget* 9(76), pp. 34413–28. doi:10.18632/oncotarget.26126.

Cavo, Marta, Marco Fato, Leonardo Peñuela, Francesco Beltrame, Roberto Raiteri, and Silvia Scaglione.,(2016). Microenvironment Complexity and Matrix Stiffness Regulate Breast Cancer Cell Activity in a 3D in Vitro Model. *Scientific Reports* 6(September), pp. 1–13. doi:10.1038/srep35367.

Chen, Rui, Shipeng Guo, Chengcheng Yang, Lu Sun, Beige Zong, Kang Li, Li Liu., (2020). Although C-MYC Contributes to Tamoxifen Resistance, It Improves Cisplatin Sensitivity in ER-Positive Breast Cancer. I*nternational Journal of Oncology* 56(4), pp. 932–44. doi:10.3892/ijo.2020.4987.

Chen, Yiting, Xueping Feng, Yuhao Yuan, Jiahui Jiang, Peihe Zhang, and Bin Zhang., (2022). Identification of a Novel Mechanism for Reversal of Doxorubicin-Induced Chemotherapy Resistance by TXNIP in Triple-Negative Breast Cancer via Promoting Reactive Oxygen-Mediated DNA Damage. *Cell Death and Disease* 13(4). doi:10.1038/s41419-022-04783-z.

Cheng, Ran, Ya Jing Liu, Jun Wei Cui, Man Yang, Xiao Ling Liu, Peng Li, Zhan Wang., (2017). Aspirin Regulation of C-MYC and CyclinD1 Proteins to Overcome Tamoxifen Resistance in Estrogen Receptor-Positive Breast Cancer Cells. *Oncotarget* 8(18), pp.30252–64. doi:10.18632/oncotarget.16325.

Debnath, Jayanta, Noor Gammoh, and Kevin M. Ryan., (2023). Autophagy and Autophagy-Related Pathways in Cancer.*Nature Reviews Molecular Cell Biology* 24(8), pp.560–75. doi:10.1038/s41580-023-00585-z.

Fallah, Yassi, Janetta Brundage, Paul Allegakoen, and Ayesha N. Shajahan-Haq.,(2017). MYC-Driven Pathways in Breast Cancer Subtypes.*Biomolecules* 7(3), pp. 1–6.

doi:10.3390/biom7030053.

Franchi, Marco, Zoi Piperigkou, Konstantinos Athanasios Karamanos, Leonardo Franchi, and Valentina Masola.,(2020). Extracellular Matrix-Mediated Breast Cancer Cells Morphological Alterations, Invasiveness, and Microvesicles/Exosomes Release. *Cells*, 9(9), pp. 1–16. doi:10.3390/cells9092031.

Gao, Fang yan, Xin tong Li, Kun Xu, Run tian Wang, and Xiao xiang Guan.,(2023). C-MYC Mediates the Crosstalk between Breast Cancer Cells and Tumor Microenvironment.*Cell Communication and Signaling*, 21(1), pp. 1–8. doi:10. 1186/ s12964-023-01043-1.

Hennig, Paulina, Gabriele Fenini, Michela Di Filippo, Tugay Karakaya, and Hans Dietmar Beer.,(2021). The Pathways Underlying the Multiple Roles of P62 in Inflammation and Cancer. *Biomedicines*, 9(7), pp. 1–19. doi:10.3390/biomedicines9070707.

Hurley, James H., and Lindsey N. Young.,(2017). Mechanisms of Autophagy Initiation. *Annual Review of Biochemistry*, (86), pp. 225–44. doi:10.1146/annurev-biochem-061516-044820.

Hutchinson, Katherine E., Mellissa J. Nixon, Mónica V. Estrada, Violeta Sánchez, Melinda E. Sanders, Taekyu Lee, Henry Gómez., (2018). MYC and MCL1 Cooperatively Promote Chemotherapy- Resistant Breast Cancer Stem Cells via Regulation of Mitochondrial Oxidative Phosphorylation. *Cell Metabolism*, 26(4), pp. 633–47. doi:10.1016/j.cmet.2017.09.009.MYC.

Jahangiri, Leila, Perla Pucci, Tala Ishola, Ricky M. Trigg, John A. Williams, Joao Pereira, Megan L. Cavanagh., (2021). The Contribution of Autophagy and Lncrnas to MYC-Driven Gene Regulatory Networks in Cancers. *International Journal of Molecular Sciences*, 22(16). doi:10.3390/ijms22168527.

Jung, Seonghee, Hyeonjeong Jeong, and Seong Woon Yu.,(2020). Autophagy as a Decisive Process for Cell Death. *Experimental and Molecular Medicine*, 52(6), pp. 921–30. doi:10.1038/s12276-020-0455-4.

Kciuk, Mateusz, Adrianna Gielecińska, Somdutt Mujwar, Damian Kołat, Żaneta Kałuzińska-Kołat, Ismail Celik, and Renata Kontek.,(2023). Doxorubicin—An Agent with Multiple Mechanisms of Anticancer Activity. *Cells*, 12(4), pp. 26–32. doi:10. 3390/cells12040659.

Lei, Cheng, Bing Zhao, Lin Liu, Xiangyue Zeng, Zhen Yu, and Xiyan Wang., (2020). Expression and Clinical Significance of P62 Protein in Colon Cancer.*Medicine (United States)* 99(3), pp. 1–6. doi:10.1097/MD.0000000000018791.

Liu, Junxia, Wei Yue, and Haiyan Chen., (2019). The Correlation between Autophagy and Tamoxifen Resistance in Breast Cancer. *International journal of clinical and experimental pathology*, 12(6), pp. 2066–74. http://www.ncbi.nlm.nih.gov/pubmed/31934028%0Ahttp://www.pubmedcentral.nih.gov/articlerender.fcgi?artid=PMC6949623.

Liu, Shizuo., (2023). Autophagy : Regulator of Cell Death.*CDDpress*. doi:10.1038/s41419-023-06154-8.

Livak, Kenneth J., and Thomas D. Schmittgen., (2001). Analysis of Relative Gene Expression Data Using Real-Time Quantitative QRT-PCR and the 2-ΔΔCT Method. *Methods* 25(4), pp. 402–8. doi:10.1006/meth.2001.1262.

Loh, Jian Sheng, Nusaibah Abdul Rahim, Yin Sim Tor, and Jhi Biau Foo., (2022). Simultaneous Proteasome and Autophagy Inhibition Synergistically Enhances Cytotoxicity of Doxorubicin in Breast Cancer Cells. *Cell Biochemistry and Function* 40(4), pp. 403–16. doi:10.1002/cbf.3704.

Lovitt, Carrie J., Todd B. Shelper, and Vicky M. Avery., (2018). Doxorubicin Resistance in Breast Cancer Cells Is Mediated by Extracellular Matrix Proteins. *BMC Cancer* 18(1), pp. 1–11. doi:10.1186/s12885-017-3953-6.

Ma, Le, Qiang Gong, Yan Chen, Peng Luo, Jieping Chen, and Chunmeng Shi., (2023). Targeting Positive Cofactor 4 Induces Autophagic Cell Death in MYC-Expressing Diffuse Large B-Cell Lymphoma. *Experimental Hematology* 119–120, pp, 42-57.e4. doi:10.1016/j.exphem.2023.01.001.

Medda, Alessandro, Micaela Compagnoni, Giorgio Spini, Simona Citro, Ottavio Croci, Stefano Campaner, Marta Tagliabue, Mohssen Ansarin, and Susanna Chiocca., (2023). C-MYC-Dependent Transcriptional Inhibition of Autophagy Is Implicated in

Cisplatin Sensitivity in HPV-Positive Head and Neck Cancer. *Cell Death and Disease* 14(11), pp.1–14. doi:10.1038/s41419-023-06248-3.

Mejlvang, Jakob, Hallvard Olsvik, Steingrim Svenning, Jack Ansgar Bruun, Yakubu Princely Abudu, Kenneth Bowitz Larsen, Andreas Brech., (2018). Starvation Induces Rapid Degradation of Selective Autophagy Receptors by Endosomal Microautophagy. *Journal of Cell Biology*, 217(10), pp. 3640–55. doi:10.1083/JCB.201711002.

Parzych, Katherine R., and Daniel J. Klionsky.,(2014). An Overview of Autophagy: Morphology, Mechanism, and Regulation. *Antioxidants and Redox Signaling*, 20(3), pp. 460–73. doi:10.1089/ars.2013.5371.

Su, Min Xia, Yu Lian Xu, Xiao Ming Jiang, Mu Yang Huang, Le Le Zhang, Luo Wei Yuan, Xiao Huang Xu., (2022). C-MYC-Mediated TRIB3/P62+ Aggresomes Accumulation Triggers Paraptosis upon the Combination of Everolimus and Ginsenoside Rh2. *Acta Pharmaceutica Sinica* B, 12(3), pp. 1240–53. doi:10.1016/j.apsb.2021.09.014.

Sun, Yi Sheng, Zhao Zhao, Zhang Nv Yang, Fang Xu, Hang Jing Lu, Zhi Yong Zhu, Wen Shi., (2017). Risk Factors and Preventions of Breast Cancer. *International Journal of Biological Sciences*, 13(11), pp. 1387–97. doi:10.7150/ijbs.21635.

Sung, Hyuna, Jacques Ferlay, Rebecca L Siegel, Mathieu Laversanne, Isabelle Soerjomataram, Ahmedin Jemal, and Freddie Bray.,(2021). Global Cancer Statistics 2020 : GLOBOCAN Estimates of Incidence and Mortality Worldwide for 36 Cancers in 185 Countries. *Cacancer Journal*, 71(3), pp. 209–49. doi:10. 3322/ caac.21660.

Thomé, Marcos P., Eduardo C. Filippi-Chiela, Emilly S. Villodre, Celina B. Migliavaca, Giovana R. Onzi, Karina B. Felipe, and Guido Lenz., (2016). Ratiometric Analysis of Acridine Orange Staining in the Study of Acidic Organelles and Autophagy. *Journal of Cell Science*, 129(24), pp. 4622–32. doi:10.1242/jcs.195057.

Toh, Pearl P C, Shouqing Luo, Fiona M Menzies, Erich E Wanker, and David C Rubinsztein., (2013). MYC Inhibition Impairs Autophagosome Formation. *Human Molecular Genetics*, 22(25), pp. 5237–48. doi:10.1093/hmg/ddt381.

Waks, Adrienne G., and Eric P. Winer., (2019). Breast Cancer Treatment: A Review. *JAMA - Journal of the American Medical Association*, 321(3), pp. 288–300. doi:10. 1001/ jama.2018.19323.

Wang, Hejing, Junmin Qian, Yaping Zhang, Weijun Xu, Juxiang Xiao, and Aili Suo., (2017). Growth of MCF-7 Breast Cancer Cells and Efficacy of Anti-Angiogenic Agents in a Hydroxyethyl Chitosan/Glycidyl Methacrylate Hydrogel. *Cancer Cell International*, 17(1), pp. 1–14. doi:10.1186/s12935-017-0424-8.

Wang, Qi, Melisa Gun, and Xing yu Hong., (2019). Induced Tamoxifen Resistance Is Mediated by Increased Methylation of E-Cadherin in Estrogen Receptor-Expressing Breast Cancer Cells. *Scientific Reports*, 9(1), pp. 3–9. doi:10.1038/s41598-019-50749-1.

Wang, Yuntao, Wei Yue, Haiyan Lang, Xiaoqing Ding, Xinyi Chen, and Haiyan Chen., (2021). Resuming Sensitivity of Tamoxifen-Resistant Breast Cancer Cells to Tamoxifen by Tetrandrine. *Integrative Cancer Therapies*, 20(6), pp. 1–9. doi:10. 1177/1534735421996822.

Yamamoto, Hayashi, Sidi Zhang, and Noboru Mizushima., (2023). Autophagy Genes in Biology and Disease. *Nature Reviews Genetics*, 24(June). doi:10.1038/s41576-022-00562-w.

Zachari, Maria, Marianna Longo, and Ian G. Ganley., (2020). Aberrant Autophagosome Formation Occurs upon Small Molecule Inhibition of ULK1 Kinase Activity. *Life Science Alliance*, 3(12), pp. 1–11. doi:10.26508/LSA.202000815.

Zhang, Yong-qu, Rong-hui Li, Wei-ling Chen, Xin Liu, Li-xin Zhang, Cui-ping Guo, Zhi-hang Huang., (2024). Autophagy Induced by Atg5 or Atg5-Atg12 Promote Tamoxifen Resistance in Breast Cancer. *Heliyon* (June). doi.org/10. 2139/ ssrn.486655

ARABIC SUMMARY

تأثير تثبيط MYC جين علي حث عملية الألتهام الذاتي الخلوى لخلايا سرطان الثدى المستجيبة و المقاومة للعلاج الكيماوى

هدي عماد الدين ورقية حسين شلبي و شيماء محمد محمود يحيي و نادية نبل داوود أنيس و شيرين حسن بدوي الوكيل
1-قسم علم الحيوان- كلية البنات للعلوم والآداب والتربية - جامعة عين شمس- شارع أسماء فهمى- هليوبوليس القاهرة- مصر
2-قسم الهرمونات معهد البحوث الطبية - مختبر الخلايا الجذعية -المركز القومي للبحوث - الدقي – الجيزة - مصر

يعتبر سرطان الثدى هو الورم الخبيث الأكثر انتشاراً بين النساء، وهو السبب الخامس الرئيسي لوفيات السرطان. يتم استخدام العلاج الجراحي والعلاج الإشعاعي والعلاج الكيميائي والعلاج المناعي معا لعلاج سرطان الثدي، حسب المرحلة ونوع الورم. ومع ذلك، لا يزال مقاومة العلاج الكيميائي تمثل مشكلة سريرية خطيرة في معالجة سرطان الثدي. في الوقت الحالي، أصبح دور الالتهام الذاتي للخلايا في مقاومة السرطان واحدًا من المجالات التي تحظى بالتحقيق المكثف. فقد تم تخطيط هذه الدراسة لتقييم معرفة تأثير تثبيط c-MYC على تحفيز الالتهام الذاتي في خلايا سرطان الثدي المستجيبة والمقاومة للعلاج الكيميائي. ولتحقيق هدف هذه الدراسة، استخدمنا نوعين مختلفين من خلايا سرطان الثدي. خلايا MCF-7الحساسة للإستروجين، المزروعة في وجود التاموكسيفين(TAM) ، و الخلايا ثلاثية السلبيةMDA-MB 231 ، المزروعة في وسط يحتوي على دوكسوروبيسين .(DOX) تم ملاحظة تغييرات في الشكل الخلوي أظهرت نمط الخلايا المقاومة للعلاج في نهاية الزراعة السابعة. كشف الميكروسكوب الفلوري أن تثبيط c-MYC يحفز قدرة الالتهام الذاتي في خلايا MCF-7 المعالجة بالتاموكسيفين، ومع ذلك، كانت الفجوات الالتهامية أعلى بكثير في خلايا MDR/MCF-7،(المقاومة للتاموكسفين) وكانت في أعلى مستوياتها في خلايا MDR- MCF-7 التي تم تثبيط c-MYC فيها. أدى تثبيط c-MYC في خلايا MDR- MDA-MB231 إلى أقوى انبعاث، أكثر من خلايا MDA-MB231 (المرجعية NC)، وأكثر من خلايا MDA-MB231 المعالجة بشكل حاد في كلا المجموعتين المختبرتين. كشف تحليل ال QRT-PCRزيادة في مستوى الجينات المتعلقة بالالتهام الذاتي في خلايا MCF-7 المعالجة بالتاموكسيفين والمثبطة لـ c-MYC، مما يشير إلى زيادة في تحفيز الالتهام الذاتي. أدى قمع c-MYC في خلايا MCF-7 المقاومة للتاموكسيفين إلى زيادة تعبير جميع الجينات المتعلقة بالالتهام الذاتي مقارنة بالخلايا المرجعية MCF-7 المقاومة للتاموكسيفين. أما بالنسبة لخلاياMDA-MB231 ، فقد اظهرت نتائج QRT-PCR زيادة مستويات جميع الجينات المتعلقة بالالتهام الذاتي في الخلايا المعالجة بشكل حاد بالدوكسوروبيسين، ومع ذلك، فإن تثبيط c-MYC قلل من تعبير معظم الجينات المتعلقة بالالتهام الذاتي. من ناحية أخرى، أدى تثبيط c-MYC في خلايا MDR/MDA-MB231 المقاومة للعلاج الكيماوى، إلى زيادة مستويات تعبير جميع الجينات المتعلقة بالالتهام الذاتي، وكانت أعلى بكثير من خلايا MDR/MDA-MB231المرجعية. وختاما قد أكدت نتائج الدراسة الحالية أن تقليل c-MYC كان له تأثيرات مختلفة على تحفيز الالتهام الذاتي اعتمادًا على نوع خلايا سرطان الثدي في الخلايا الحساسة للعلاج الكيميائي؛ حيث وجد أنه ارتفع في خلاياMCF-7 ، بينما انخفض في خلايا MDA-MB 231 ومع ذلك، فإنه يرفع بشكل واضح الالتهام الذاتي في الخلايا المقاومة للتاموكسيفين والدوكسوروبيسين.